

# **Track-and-Trace: Novel Anti-Counterfeit Measures for 3D Printed Personalised Drug Products using Smart Material Inks**

Sarah J Trenfield<sup>1</sup>, Hui Xian Tan<sup>1</sup>, Atheer Awad<sup>1</sup>, Asma Buanz<sup>1</sup>, Simon Gaisford<sup>1,2</sup>, Abdul W Basit<sup>1,2\*</sup> and Alvaro Goyanes<sup>2\*</sup>.

<sup>1</sup>UCL School of Pharmacy, University College London, 29-39 Brunswick Square, London WC1N 1AX, UK

<sup>2</sup>FabRx Ltd., 3 Romney Road, Ashford, Kent, TN24 0RW, UK

\*Correspondence: [a.basit@ucl.ac.uk](mailto:a.basit@ucl.ac.uk) (Abdul W. Basit)

[a.goyanes@FabRx.co.uk](mailto:a.goyanes@FabRx.co.uk) (Alvaro Goyanes)

## **Abstract**

Printing technologies have been forecast to initiate a new era of personalised medicine in pharmaceuticals. To facilitate integration, a non-destructive and robust method of product authenticity is required. This study reports, for the first time, the interface between 3D printing and 2D inkjet printing technologies in order to fabricate a drug-loaded 3D printed tablet (printlet) with a unique track-and-trace measure in a single step process. In particular, quick response (QR) codes and data matrices were printed onto the surface of polymeric-based printlets for scanning using a smartphone device, and were designed to encode tailored information pertaining to the drug product, patient and prescriber. Moreover, a novel anti-counterfeit strategy was designed, which involved the deposition of a unique combination of material inks for detection using Raman spectroscopy. The inks were characterised for printability by measuring surface tension, viscosity and density, and each were successfully detected on the 3D printed tablet post-printing. Overall, this novel approach will enable an enhanced transparency and tracking of 3D printed medicines across the supply chain, leading to a safer treatment pathway for patients.

## **Key words**

Three-dimensional printing; falsified medicines; additive manufacturing; ink-jet printing; counterfeit medicines; 3D printed drug products

## 1. Introduction

Substandard or falsified medicines pose a serious threat to global public health. According to the World Health Organization (WHO), 10.5% of low- and middle-income countries are imposed by substandard or falsified medicines, costing an estimated US\$ 30.5 billion annually (Kelesidis and Falagas, 2015; WHO, 2018). In sub-Saharan Africa alone, counterfeit anti-malarials are found to contribute up to an additional 267,000 deaths annually (Naughton, 2018). It is clear that the development of effective anti-counterfeit strategies is required to maintain patient safety across the pharmaceutical supply chain (Han et al., 2012; You et al., 2016).

As a result of global initiatives such as the European Union Falsified Medicines Directive and the US Drug Supply Chain Security Act (EU, 2011; FDA, 2013), pharmaceutical manufacturers and suppliers are looking towards adopting a worldwide standardised identification system to support product traceability and combat drug counterfeiting. Current authentication strategies utilise two main strategies: 1) use of tamper-evident or –resistant packaging; and 2) serialisation of packaging i.e. printing of two-dimensional (2D) barcodes (Bansal et al., 2013; EMA, 2016). However, these strategies would likely only be suitable for those medicines that are manufactured *en masse*, in the presence of specialised packaging.

In the case of personalised medicines, whereby small or ‘one-off’ batches of tailored dosage forms are produced for on demand administration, a novel authentication method is required (Nørfeldt et al., 2019). Printing technologies

have been widely explored over the last decade for production of personalised medicines (Alhnan et al., 2016; Awad et al., 2019; Awad et al., 2018a; Basit and Gaisford, 2018; Fina et al., 2018; Sadia et al., 2018). The most widely researched three-dimensional (3D) printing technology is fused deposition modeling (FDM), whereby a drug-loaded filament is extruded through a heated nozzle for deposition onto a build platform, layer-by-layer (Awad et al., 2018a; Kollamaram et al., 2018; Melocchi et al., 2016; Zhang et al., 2017). Moreover, 2D inkjet printing technologies enable a precise spatial control over droplet ejection, enabling small and personalised dosages and patterns to be deposited onto oral substrates (Alomari et al., 2018; Buanz et al., 2011; Edinger et al., 2018; Edinger et al., 2019; Sandler and Preis, 2016; Thabet et al., 2018; Vuddanda et al., 2018; Wickström et al., 2018).

Due to their compact size, affordability and flexibility, printing processes are highly suitable for the production of tailored medicines in decentralised locations, such as at the point-of-care or within localised special manufacturing facilities (Awad et al., 2018b; Robles-Martinez et al., 2019; Trenfield et al., 2018a). As such, it is likely that 3D printed personalised medicines would be produced in the absence of specialised anti-counterfeit packaging. In this instance, it would be more favourable to include an authentication measure directly on the dosage form. Due to their relatively simple internal graphic design, codes such as data matrices and quick response (QR) codes have previously been included directly onto the surface or imbedded within small dosage forms (Chen et al., 2018; Edinger et al., 2018; Fei and Liu, 2016). Favourably, these codes can encode a host of

product information, such as the drug name, dosage, patient name, prescriber details, etc. ready for scanning using a handheld smartphone device before administration (Edinger et al., 2018; Liang et al., 2012). Application of a barcode directly on the dosage form have been indicated for preventing counterfeiting of medicine (You et al., 2016), as well as improving medication safety and adherence and reduction of visits to healthcare professionals by enabling clinicians and patients to monitor digitally (Mira et al., 2015; Rathbone and Prescott, 2017).

However, as 2D barcodes are visible they pose the risk of duplication and, as such, combination with a covert (or invisible) anti-counterfeit method could be used to ensure product authenticity. This concept was demonstrated in the case of SmartWater™, whereby a unique combination of detectable ingredients are deposited onto goods, aiding in asset traceability and to deter theft (Cleary, 1998). This strategy could be applied to pharmaceuticals; using inkjet printing, a unique combination of pharmaceutically approved materials could be deposited onto the printlet surface according to a randomised anti-counterfeit code. The deposited materials could then be scanned and identified using Raman spectroscopy, which is a non-destructive and rapid detection method widely explored for its use in anti-counterfeit applications (Kakio et al., 2017; Lawson et al., 2018; Mazivila and Olivieri, 2018; Trenfield et al., 2018b).

To this end, the aims of this project were, for the first time, to evaluate the use of dual FDM 3D printing and 2D inkjet printing technologies. To date, these

technologies have been used separately, whereby 3D printed constructs require removal from the build platform and inserted into an inkjet printer for coating or ink deposition (Krivec et al., 2017). Here, we have instead combined these printing technologies to fabricate a drug-loaded personalised medicine with a combined track-and-trace identifier (QR code or data matrix) and anti-counterfeit method (deposited material inks) in a single step process. This concept seeks to serve two-fold purposes: 1) to ensure that the 3D printed drug product is genuine; and 2) to be assigned to an individual patient at the point of production to enable transparency and tracking.

## **2. Materials and Methods**

### **2.1. Materials**

Paracetamol USP grade (Sigma-Aldrich, Co. Ltd., UK) was used as a model drug (BCS Class I, high solubility and high permeability, molecular weight: 151.16, solubility in water at 25°C: 14 mg/mL) (Yalkowsky et al., 2003). For anti-counterfeit model production, commercial polylactic acid (PLA) 1.75 mm filaments (XYZ printing, NE) or polyvinyl acetate (PVA) 1.75 mm filaments were purchased (Makerbot Inc. USA). For the production of paracetamol-loaded filaments, L-hydroxypropylcellulose (L-HPC; Nisso™, US) was used as the polymer, mannitol (Sigma-Aldrich Co. Ltd., UK) was used as a plasticiser and magnesium stearate (Sigma-Aldrich Co. Ltd., UK) was used as a lubricant. The following materials were evaluated for suitability of anti-counterfeit code deposition: methylparaben (VWR Life Science, US), Eudragit RS100 (Evonik, US) and sodium benzoate (Sigma-Aldrich Co. Ltd., UK). Fluorescein sodium (Fluka, Sigma-Aldrich Co. Ltd., UK) was used as a

dye to indicate printability. Solvents used for ink preparation included ethylmethylketone (Fischer Scientific, UK), acetone (Sigma-Aldrich Co. Ltd., UK) and methanol (Sigma-Aldrich Co. Ltd., UK).

## **2.2. Filament preparation**

Paracetamol (5%), L-HPC (75%), mannitol (15%) and magnesium stearate (5%) were mixed in a pestle and mortar until an absence of polymer agglomeration. The mixture was then extruded using a single-screw filament extruder (Noztec Pro Hot Melt Extruder; Noztec, UK) in order to obtain a filament suitable for printing (temperature 150°C, nozzle diameter 1.75 mm, screw speed 15 rpm). The extruded filaments were stored protected from light.

## **2.3. Designs and Printing of Tablets**

Printlet 3D models were designed using XYZ Maker software, comprising a centralised QR code or a data matrix and surrounded by four coloured dots (representing the regions of material deposition) as an example anti-counterfeit tablet model (Figure 1). In particular, a pure black circle (RGB: 0,0,0), a pure cyan circle (RGB: 0,255,255), a pure magenta circle (RGB: 255,0,255) and a pure yellow circle (RGB: 255,255,0) were created using Adobe Photoshop software (Adobe, Co. Ltd., US) and were applied on the top of the printlet by using the 'Sketch 3D' function within the software.

A Da Vinci Color 3D printer (XYZ Printing, US) was used in this study, which is a full colour 3D printer that combines fused deposition modelling (FDM) and piezoelectric 2D inkjet printing technology in order to fabricate

objects of designed colours and patterns. All printlets were printed at 210°C in a mode of high printing detail and slow printhead moving speed. The minimal printing layer height of tablets was 0.1 mm.

A variety of diameters (10mm, 12 mm and 15 mm) and tablet heights (1 mm and 3.6 mm) were designed and evaluated for ease of scanning using a smart phone QR code and data matrix reader (QR Reader for iPhone, Tapmedia Ltd, UK).

## **2.4. 2D barcode generation**

Data matrices and QR codes containing the required information were prepared using an online code generator (<http://datamatrix.kaywa.com/> and <https://www.qr-code-generator.com/>, respectively). The matrices were encoded to direct to a website address that contained a designated 'anti-counterfeit code', which determined the positions of material deposition (positions 1 to 4; with position 1 being above the QR code or data matrix and moving in a clockwise direction to positions 2-4; Figure 1). Furthermore, personalised information relating to the printlet (such as the active ingredient, dose, batch and expiry date) and that of the patient (such as name, date of birth, gender) were encoded (Figure 2).

## **2.5. Material ink preparation**

The inks were prepared by dissolving each material, namely methylparaben (20% w/v), Eudragit RS100 (10% w/v) and sodium benzoate (2% w/v) into a mixture of ethylmethylketone, acetone and methanol (50:20:30). To aid with

development of optimised inks, the printability was calculated by using the following equation (1):

$$Z = \frac{(\alpha\rho\gamma)^{1/2}}{\eta} \quad (1)$$

Where  $Z$  represents printability of the ink;  $\alpha$ ,  $\rho$ ,  $\gamma$ , and  $\eta$  are the radius of the cartridge orifices ( $\mu\text{m}$ ), the density ( $\text{gm}^{-3}$ ), surface tension ( $\text{mNm}^{-1}$ ) and viscosity ( $\text{mPa}\cdot\text{s}$ ) of the ink, respectively (Fromm, 1984). Stable drop formation has been found to be achieved when the  $Z$  value of an ink is between 1 and 10 (Derby and Reis, 2003).

## 2.6. Surface Tension Measurements

Measurement of the inks was performed using a Kibron Delta 8 multi-channel microtensiometer (Kibron Inc, Finland) using 50  $\mu\text{L}$  of the sample solution to fill each well of the DynePlate ( $n = 8$ ). The measurement involves withdrawing a probe from the solution and recording the maximum force exerted on the surface tension (maximum pull force method). Data were captured with the Delta-8 Instrument Setup software and calibration was performed prior to measurement using distilled water as a reference (surface tension =  $72.8 \text{ mNm}^{-1}$  at  $20^\circ\text{C}$ ) in accordance with the manufacturer's instructions. Data are presented as mean  $\pm$  SD.

## **2.7. Dynamic Viscosity Measurements**

An automated viscometer (AMVn) and an 'mf MS 1.6' measuring system set was used to undertake viscosity measurements at 25°C (n = 5). This measuring system set included a capillary with a diameter of 1.6 mm which was suitable for viscosity measurements between 0.3-10 mPa.s. A small golden ball was injected into the capillary and moved under gravity through the capillary held at a 50° angle. To calculate the viscosity, the time required for the ball to pass between two marks on the capillary was measured. The viscosities of solutions were calculated with reference to data for the densities of solutions. Data are presented as mean  $\pm$  SD.

## **2.8. Modification of ink cartridges**

All experiments were performed with an unmodified Da Vinci Color Printer (XYZ Printing, NE). Ink cartridges (cyan, magenta and yellow) were modified by removing the rubber plug cover at the top and impaling the plug with a syringe to remove the original inks. The cartridges were flushed repeatedly with distilled water and absolute ethanol (50:50) until clean. The cartridges were loaded with the appropriate inks to be jetted and replaced in the carrier in the printer. In particular, methylparaben 20% ink was filled into the cyan cartridge, Eudragit RS100 10% ink into the magenta cartridge and the sodium benzoate 2% ink into the yellow. The inks were then printed on either a 12 mm tablet (for data matrix) or 15 mm tablet (for QR codes) according to the anti-counterfeit designs. In particular, positions 1 and 3 were Eudragit RS100, position 2 was methylparaben and position 4 was sodium benzoate.

Initial printability was indicated by printing a test page consisting of vertical and horizontal lines of a specific colour. After each use, the cartridge was rinsed with distilled water and absolute ethanol (50:50) until clean.

## **2.9. Raman Spectroscopy**

Raman spectroscopy was performed to evaluate the presence of material inks on the printlet surface. The topside surface of samples were mounted and focused using a X50 objective on an InVia confocal Raman microscope (Renishaw, UK) equipped with a 300 mW 785 nm HPNIR Renishaw laser at 100% laser power. A 1200 line grating was used providing spectral resolution up to  $1 \text{ cm}^{-1}$ . Spectra were collected over the range of  $100 - 3200 \text{ cm}^{-1}$ , with a 10 second exposure time and 1 accumulation. Data analysis was performed using MATLAB software version R2017a (The MathWorks, CA, USA).

## **3. Results and Discussion**

For the first time, it was possible to modify a combined 2D ink jet and 3D printer in order to fabricate a drug-loaded printlet with a unique anti-counterfeit mechanism. The Da Vinci Color printer used in this study is a full colour 3D printer that combines fused deposition modelling (FDM) and piezoelectric 2D inkjet printing technology in order to fabricate objects of designed colours and patterns (Figure 3). The commercial printer functions by extruding a colour-absorbing PLA filament through a heated nozzle (0.4 mm diameter;  $210^{\circ}\text{C}$ ) which is deposited onto a build platform in a layer-by-layer

manner. Four piezoelectric ink cartridges (cyan, yellow, magenta and black; CYMK) are situated directly above the extrusion nozzle to enable coloured ink deposition onto the filament post-printing. Upon an applied voltage, a piezoelectric material deforms within the inkjet printhead causing the ink to be ejected from the print nozzle as a droplet (Alomari et al., 2015; Scoutaris et al., 2011).

The commercial printer was modified in order to print pharmaceutical filaments and inks. In particular, loading and printing of an alternative commercially produced PVA filament as well as a drug-loaded filament (paracetamol 5% w/w and L-HPC) was performed, which are materials that have been used in other pharmaceutical studies for the production of dosage forms (Goyanes et al., 2014; Goyanes et al., 2015a; Goyanes et al., 2015b; Skowyra et al., 2015).

### **3.1. Optimisation of 2D Barcode Scanning**

During initial optimisation, the commercial CYMK inks were used to print an anti-counterfeit QR code or data matrix design on top of placebo PVA printlets. The 2D printed codes were encoded such that upon scanning it would direct the user to a webpage address containing the relevant anti-counterfeit code, as well as the personalised medication and prescribing information. The inks were found to deposit well and were not removed upon wiping or washing with distilled water.

Previous studies have shown that the size and resolution of printed QR codes and data matrices can directly affect their ease of scanning and hence

information retrieval (Kato et al., 2011). As such, it was hypothesised that the tablet diameter might directly affect the ease of code scanning. To evaluate this, a variety of different sized diameter printlets were produced (10 mm, 12 mm and 15 mm) and the minimum tablet diameter that enabled scanning of the printed QR codes and data matrices was evaluated (Figure 4). It was found that the minimum size that could be scanned by a smartphone for QR codes was 15 mm and for the data matrix was 12 mm.

The ease of scanning of the printed QR codes and data matrices was limited by the size of the jetted barcodes. For example, although the same information was encoded, the generated data matrix was inherently less complex in internal graphics structure than the generated QR code. Previous studies have demonstrated that data matrices occupy 30-60% less space than their QR code counterparts when encoding the same information (Falas and Kashani, 2007). This made it possible for data matrix to be read when printed onto the surface of the 12 mm tablet compared with the QR code. Favourably, after 6 months of storage at ambient conditions, all printlet barcodes were able to scan and retrieve the information in the QR code and data matrix.

Importantly, the size of the dosage form could also affect the ease of oral administration from a patient perspective. Ease of scanning and reduction of dosage form diameter could be further improved if the resolution of the inkjet printing process was increased; the commercial Da Vinci Color printer is designed to print medium to large-sized objects whereby high resolution is not needed. To be suitable for pharmaceutical applications, the printer would

have to be modified further to make it more suitable for printing on smaller sized objects (e.g. tablets, capsules or medical devices), where a high resolution is of utmost importance to enable a precise and controlled deposition of material.

Conventionally, QR codes and data matrices are printed in black on commercial packaging. However, with the flexibility of inkjet printing in combination with FDM 3DP, it is feasible to print such codes in a variety of colours. To evaluate the impact of colour selection on ease of scanning, cyan and yellow QR code and data matrices were printed onto printlets (diameters: 15 mm and 20 mm). For the cyan colour, it was found that the minimum scanning size for QR codes was 20 mm and for data matrices was 15 mm. For the yellow colour, neither sizes could be identified nor scanned. A similar occurrence has been observed in previous studies, whereby a reduction in contrast between the printed barcode and the white background negatively affected the ease of barcode scanning using a barcode scanner (Omerasevic et al., 2014).

### **3.2. Development of Anti-Counterfeit Material Inks**

If 3D printers were being used away from the clinic (i.e. in a centralised specials manufacturing hub for shipping to patients), the use of an anti-counterfeit measure is warranted. Previous studies have highlighted the risk of duplication of 2D barcodes if being used alone (Edinger et al., 2018). As such, we propose developing a covert material ink deposition method to overcome such challenges whereby a randomised anti-counterfeit code is

assigned to each printlet for scanning using Raman spectroscopy. Surface tension and viscosity have previously been found to be the most critical parameters when optimising inks for printing to enable stable drop formation (Alomari et al., 2015; Clark et al., 2017; de Gans et al., 2004). The original CYMK inks were found to have dynamic viscosity measurements around the values of 0.9 - 1.0 mPa.s and surface tension values in the range of 25 - 28 mNm<sup>-1</sup> (Table 1). As such, the developed material inks were at first optimised by varying the solvent ratios to achieve surface tension and dynamic viscosity values that fell in the range of the original inks. The solvent combination that was found to achieve inks that were within the range of surface tension was ethylmethylketone, methanol and acetone at a ratio of 50:30:20.

As well as the surface tension and viscosity of the ink, the size of the nozzle orifice is highly influential on the printability (Jang et al., 2009). As such, scanning electron microscopy (SEM) imaging was used to evaluate the orifice size of the inkjet printer head nozzles. The black, cyan, magenta and yellow nozzle orifice sizes were found to be 35 µm, 35 µm, 37.5 µm and 40 µm, respectively. The differences in nozzle orifice sizes have been observed in other studies and depend on nature of the colourant inks (e.g. present as either a solution or suspension, and particle size of suspended pigments). This suggests that the cartridges may be employed to jet alternative liquids, as long as the particles are solubilised in the solvent mixture or if the diameters of the dispersed particles are smaller than that of the orifices (Buanz et al., 2011).

To aid with development of the optimised inks, printability was assessed by calculating the Z value (Equation 1), taking into account the nozzle orifice size, ink surface tension, ink viscosity and ink density (Fromm, 1984). Stable drop formation has been found to only occur when the value of Z is between 1 and 10 (Derby and Reis, 2003; Jang et al., 2009). For the original CYMK inks, the Z value was ~ 4, indicating their printability. For each of the inks, the Z value was found to be 3.58, 1.15 and 4.58 for methylparaben 20% w/v, Eudragit RS100 10% w/v and sodium benzoate 2% w/v inks, respectively. Despite remaining in the printable range, the Eudragit RS100 ink exhibited a lower Z value compared with the other excipients. This was attributed to Eudragit RS100 presence increasing ink viscosity, likely due to the fact that Eudragit RS100 has a larger molecular mass (32,000 g/mol) compared with the other excipients (sodium benzoate: 144.1 g/mol; and methylparaben: 152.2 g/mol). Buanz *et al.* have previously demonstrated that viscosity is the most critical parameter for printability; as the viscosity of their ink formulations was increased, the consistency of the amount of the drug printed was reduced (Buanz et al., 2011).

Printability of the inks were evaluated using Raman microscopy, whereby the printlets were affixed onto a stage and viewed under white light at an x50 optical zoom. Each of the three inks were visually detected on the printlet surface post-printing (Figure 5).

### 3.3. Material Ink Detection with Raman Spectroscopy

Raman spectroscopy is commonly used as a material identification method in pharmaceuticals due to the generation of spectra with characteristic peaks that can be attributed to functional groups within the drug or excipient molecular structure. Furthermore, the method is inherently non-destructive, rapid and user friendly, which would likely be suitable for use on printlets in the pharmaceutical supply chain (Chen et al., 2017; Edinger et al., 2017; Rebiere et al., 2018; Trenfield et al., 2018b). As such, the use of Raman spectroscopy was evaluated for the identification of material inks on the surface of the printlets.

Initially, the pure materials (sodium benzoate, methylparaben and Eudragit RS100), as well as a blank polymeric-based printlet, were scanned in order to identify peaks of interest that could satisfy the following criteria: 1) do not overlap with the printlet peaks; and 2) have high enough sensitivity for material detection in the printed inks. For sodium benzoate, a sharp peak with high intensity was recorded at  $1006\text{ cm}^{-1}$ , which has been described in the literature (Figure 6) (De Veij M, 2009). Methylparaben showed three main regions of interests; two sharp peaks at  $858\text{ cm}^{-1}$  and  $1285\text{ cm}^{-1}$ , and a region of peaks with unique morphology at  $157\text{ cm}^{-1} - 1635\text{ cm}^{-1}$  (ChemicalBook, 2017). Eudragit RS100 was found to have a sharp peak at  $812\text{ cm}^{-1}$  (Figure 6). Once the peaks of interest had been identified, positions 1-4 on the printlet surface were scanned using Raman spectroscopy to evaluate material identification.

Favourably, for all four materials, the previously identified peaks were detected among the background blank printlet peaks (Figure 7A), demonstrating the ability for a spectroscopic approach to identify and classify the smart material inks as a novel anti-counterfeit strategy. The dual track-and-trace and anti-counterfeit method demonstrated here could transform the way that printing technologies are utilised in healthcare, providing a more streamline and robust method of product tracking and authentication across the supply chain, and leading to a safer treatment pathway for patients.

#### **4. Conclusions**

This study was the first to combine 2D and 3D printing technologies to produce a drug-loaded printlet with a dual track-and-trace and anti-counterfeit mechanism. QR codes and data matrices were successfully printed onto the printlet surfaces, which were suitable for scanning with a smartphone device to provide tailored information about the drug product, patient and prescriber. A novel anti-counterfeit mechanism was devised which involved the deposition of a unique combination of materials, which were successfully detected using Raman spectroscopy. This dual printing process could have benefits for the tracking of personalised medicines across the distribution chain: from prescription through to administration and adherence. However, the inclusion of a data matrix or QR code on the printlet surface could have an impact on the visual appearance and affect the acceptance of medication by patients. As such, this should be evaluated in clinical studies in the future. Favourably, by increasing the plethora of excipients and/or colouring agents within the material inks, the randomised code could cover millions of

combinations, facilitating the integration of personalised medicines via an improved tracking and authentication system across the supply chain.

## **5. Acknowledgements**

The authors thank the Engineering and Physical Sciences Research Council (EPSRC), UK for their financial support (EP/L01646X).

## 6. References

- Alhnan, M.A., Okwuosa, T.C., Sadia, M., Wan, K.W., Ahmed, W., Arafat, B., 2016. Emergence of 3D Printed Dosage Forms: Opportunities and Challenges. *Pharm Res* 33, 1817-1832.
- Alomari, M., Mohamed, F.H., Basit, A.W., Gaisford, S., 2015. Personalised dosing: Printing a dose of one's own medicine. *International Journal of Pharmaceutics* 494, 568-577.
- Alomari, M., Vuddanda, P.R., Trenfield, S.J., Dadoo, C.C., Velaga, S., Basit, A.W., Gaisford, S., 2018. Printing T3 and T4 oral drug combinations as a novel strategy for hypothyroidism. *International Journal of Pharmaceutics* 549, 363-369.
- Awad, A., Fina, F., Trenfield, S.J., Patel, P., Goyanes, A., Gaisford, S., Basit, A.W., 2019. 3D Printed Pellets (Miniprintlets): A Novel, Multi-Drug, Controlled Release Platform Technology. *Pharmaceutics* 11, 148.
- Awad, A., Trenfield, S.J., Gaisford, S., Basit, A.W., 2018a. 3D printed medicines: A new branch of digital healthcare. *International Journal of Pharmaceutics* 548, 586-596.
- Awad, A., Trenfield, S.J., Goyanes, A., Gaisford, S., Basit, A.W., 2018b. Reshaping drug development using 3D printing. *Drug Discovery Today* 23, 1547-1555.
- Bansal, D., Malla, S., Gudala, K., Tiwari, P., 2013. Anti-counterfeit technologies: a pharmaceutical industry perspective. *Scientia pharmaceutica* 81, 1-13.
- Basit, A., Gaisford, S., 2018. 3D Printing of Pharmaceuticals. DOI: <https://doi.org/10.1007/978-3-319-90755-0>. Springer.
- Buanz, A.B., Saunders, M.H., Basit, A.W., Gaisford, S., 2011. Preparation of personalized-dose salbutamol sulphate oral films with thermal ink-jet printing. *Pharm Res* 28, 2386-2392.
- ChemicalBook, 2017. Methylparaben (99-76-3).
- Chen, D.-D., Xie, X.-F., Ao, H., Liu, J.-L., Peng, C., 2017. Raman spectroscopy in quality control of Chinese herbal medicine. *Journal of the Chinese Medical Association* 80, 288-296.

Chen, F., Luo, Y., Tsoutsos, N.G., Maniatakos, M., Shahin, K., Gupta, N., 2018. Embedding Tracking Codes in Additive Manufactured Parts for Product Authentication. *Advanced Engineering Materials* 0, 1800495.

Clark, E.A., Alexander, M.R., Irvine, D.J., Roberts, C.J., Wallace, M.J., Sharpe, S., Yoo, J., Hague, R.J.M., Tuck, C.J., Wildman, R.D., 2017. 3D Printing of Tablets Using Inkjet with UV Photoinitiation. *International Journal of Pharmaceutics* 529, 523-530.

Cleary, M., 1998. Method of identifying a surface. Smartwater Ltd.

de Gans, B.J., Duineveld, P.C., Schubert, U.S., 2004. Inkjet Printing of Polymers: State of the Art and Future Developments. *Advanced Materials* 16, 203-213.

De Veij M, V.P., De Beer T, Remon JP, Moens L, 2009. Reference database of Raman spectra of pharmaceutical excipients. *Journal of Raman Spectroscopy* 40, 297-307.

Derby, B., Reis, N., 2003. Inkjet Printing of Highly Loaded Particulate Suspensions. *MRS Bulletin* 28, 815-818.

Edinger, M., Bar-Shalom, D., Rantanen, J., Genina, N., 2017. Visualization and Non-Destructive Quantification of Inkjet-Printed Pharmaceuticals on Different Substrates Using Raman Spectroscopy and Raman Chemical Imaging. *Pharmaceutical Research* 34, 1023-1036.

Edinger, M., Bar-Shalom, D., Sandler, N., Rantanen, J., Genina, N., 2018. QR encoded smart oral dosage forms by inkjet printing. *International Journal of Pharmaceutics* 536, 138-145.

Edinger, M., Iftimi, L.-D., Markl, D., Al-Sharabi, M., Bar-Shalom, D., Rantanen, J., Genina, N., 2019. Quantification of Inkjet-Printed Pharmaceuticals on Porous Substrates Using Raman Spectroscopy and Near-Infrared Spectroscopy. *AAPS PharmSciTech* 20, 207.

EMA, 2016. Falsified Medicines.

EU, 2011. Directive 2011/62/EU of the European Parliament and of the Council

Falas, T., Kashani, H., 2007. Two-Dimensional Bar-Code Decoding with Camera-Equipped Mobile Phones, Fifth Annual IEEE International Conference on Pervasive Computing and Communications Workshops (PerComW'07), pp. 597-600.

FDA, 2013. Drug Supply Chain Security Act.

Fei, J., Liu, R., 2016. Drug-laden 3D biodegradable label using QR code for anti-counterfeiting of drugs. *Materials Science and Engineering: C* 63, 657-662.

Fina, F., Goyanes, A., Madla, C.M., Awad, A., Trenfield, S.J., Kuek, J.M., Patel, P., Gaisford, S., Basit, A.W., 2018. 3D printing of drug-loaded gyroid lattices using selective laser sintering. *International Journal of Pharmaceutics* 547, 44-52.

Fromm, J.E., 1984. Numerical Calculation of the Fluid Dynamics of Drop-on-Demand Jets. *IBM Journal of Research and Development* 28, 322-333.

Goyanes, A., Buanz, A.B.M., Basit, A.W., Gaisford, S., 2014. Fused-filament 3D printing (3DP) for fabrication of tablets. *International Journal of Pharmaceutics* 476, 88-92.

Goyanes, A., Buanz, A.B.M., Hatton, G.B., Gaisford, S., Basit, A.W., 2015a. 3D printing of modified-release aminosalicylate (4-ASA and 5-ASA) tablets. *Eur J Pharm Biopharm* 89, 157-162.

Goyanes, A., Chang, H., Sedough, D., Hatton, G.B., Wang, J., Buanz, A., Gaisford, S., Basit, A.W., 2015b. Fabrication of controlled-release budesonide tablets via desktop (FDM) 3D printing. *International Journal of Pharmaceutics* 496, 414-420.

Han, S., Bae Hyung, J., Kim, J., Shin, S., Choi, S.-E., Lee Sung, H., Kwon, S., Park, W., 2012. Lithographically Encoded Polymer Microtaggant Using High-Capacity and Error-Correctable QR Code for Anti-Counterfeiting of Drugs. *Advanced Materials* 24, 5924-5929.

Jang, D., Kim, D., Moon, J., 2009. Influence of Fluid Physical Properties on Ink-Jet Printability. *Langmuir* 25, 2629-2635.

Kakio, T., Yoshida, N., Macha, S., Moriguchi, K., Hiroshima, T., Ikeda, Y., Tsuboi, H., Kimura, K., 2017. Classification and Visualization of Physical and Chemical Properties of Falsified Medicines with Handheld Raman Spectroscopy and X-Ray Computed Tomography. *The American Journal of Tropical Medicine and Hygiene* 97, 684-689.

Kato, Y., Deguchi, D., Takahashi, T., Ide, I., Murase, H., 2011. Low Resolution QR-Code Recognition by Applying Super-Resolution Using the

Property of QR-Codes, 2011 International Conference on Document Analysis and Recognition, pp. 992-996.

Kelesidis, T., Falagas, M.E., 2015. Substandard/Counterfeit Antimicrobial Drugs. *Clinical Microbiology Reviews* 28, 443-464.

Kollamaram, G., Croker, D.M., Walker, G.M., Goyanes, A., Basit, A.W., Gaisford, S., 2018. Low temperature fused deposition modeling (FDM) 3D printing of thermolabile drugs. *Int J Pharm* 545, 144-152.

Krivec, M., Roshanghias, A., Abram, A., Binder, A., 2017. Exploiting the combination of 3D polymer printing and inkjet Ag-nanoparticle printing for advanced packaging. *Microelectronic Engineering* 176, 1-5.

Lawson, G., Ogwu, J., Tanna, S., 2018. Quantitative screening of the pharmaceutical ingredient for the rapid identification of substandard and falsified medicines using reflectance infrared spectroscopy. *PLOS ONE* 13, e0202059.

Liang, K., Thomasson, J.A., Lee, K.-M., Shen, M., Ge, Y., Herrman, T.J., 2012. Printing data matrix code on food-grade tracers for grain traceability. *Biosystems Engineering* 113, 395-401.

Mazivila, S.J., Olivieri, A.C., 2018. Chemometrics coupled to vibrational spectroscopy and spectroscopic imaging for the analysis of solid-phase pharmaceutical products: A brief review on non-destructive analytical methods. *TrAC Trends in Analytical Chemistry* 108, 74-87.

Melocchi, A., Parietti, F., Maroni, A., Foppoli, A., Gazzaniga, A., Zema, L., 2016. Hot-melt extruded filaments based on pharmaceutical grade polymers for 3D printing by fused deposition modeling. *International Journal of Pharmaceutics* 509, 255-263.

Mira, J., Guilabert, M., Carrillo, I., Fernandez, C., Vicente, M., Orozco-Beltran, D., Gil-Guillen, V., 2015. Use of QR and EAN-13 codes by older patients taking multiple medications for a safer use of medication. *Int J Med Inf* 84, 406-412.

Naughton, B., 2018. The future of falsified and substandard medicine detection: digital methods to track and authenticate pharmaceutical products. Pathways for Prosperity Commission

Nørfeldt, L., Bøtker, J., Edinger, M., Genina, N., Rantanen, J., 2019. Cryptopharmaceuticals: Increasing the Safety of Medication by a Blockchain of Pharmaceutical Products. *Journal of Pharmaceutical Sciences*

Omerasevic, D., Behlilovic, N., Mrdovic, S., 2014. An implementation of secure key exchange by using QR codes, *Proceedings ELMAR-2014*, pp. 1-4.

Rathbone, A., Prescott, J., 2017. The Use of Mobile Apps and SMS Messaging as Physical and Mental Health Interventions: Systematic Review. *J Med Internet Res* 19, 295.

Rebiere, H., Martin, M., Ghyselincq, C., Bonnet, P.-A., Brenier, C., 2018. Raman chemical imaging for spectroscopic screening and direct quantification of falsified drugs. *Journal of pharmaceutical and biomedical analysis* 148, 316-323.

Robles-Martinez, P., Xu, X., Trenfield, S.J., Awad, A., Goyanes, A., Telford, R., Basit, A.W., Gaisford, S., 2019. 3D Printing of a Multi-Layered Polypill Containing Six Drugs Using a Novel Stereolithographic Method. *Pharmaceutics* 11, 274.

Sadia, M., Arafat, B., Ahmed, W., Forbes, R.T., Alhnan, M.A., 2018. Channelled tablets: An innovative approach to accelerating drug release from 3D printed tablets. *J Control Release* 269, 355-363.

Sandler, N., Preis, M., 2016. Printed Drug-Delivery Systems for Improved Patient Treatment. *Trends in pharmacological sciences* 37, 1070-1080.

Scoutaris, N., Alexander, M.R., Gellert, P.R., Roberts, C.J., 2011. Inkjet printing as a novel medicine formulation technique. *Journal of Controlled Release* 156, 179-185.

Skowyra, J., Pietrzak, K., Alhnan, M.A., 2015. Fabrication of extended-release patient-tailored prednisolone tablets via fused deposition modelling (FDM) 3D printing. *Eur J Pharm Sci* 68, 11-17.

Thabet, Y., Lunter, D., Breitzkreutz, J., 2018. Continuous inkjet printing of enalapril maleate onto orodispersible film formulations. *International Journal of Pharmaceutics* 546, 180-187.

Trenfield, S.J., Awad, A., Goyanes, A., Gaisford, S., Basit, A.W., 2018a. 3D Printing Pharmaceuticals: Drug Development to Frontline Care. *Trends in pharmacological sciences* 39, 440-451.

Trenfield, S.J., Goyanes, A., Telford, R., Wilsdon, D., Rowland, M., Gaisford, S., Basit, A.W., 2018b. 3D printed drug products: Non-destructive dose verification using a rapid point-and-shoot approach. *International Journal of Pharmaceutics* 549, 283-292.

Vuddanda, P.R., Alomari, M., Dodoo, C.C., Trenfield, S.J., Velaga, S., Basit, A.W., Gaisford, S., 2018. Personalisation of warfarin therapy using thermal ink-jet printing. *European Journal of Pharmaceutical Sciences* 117, 80-87.

WHO, 2018. Growing threat from counterfeit medicine.

Wickström, H., Broos, A., Nyman, J.O., Kortesmäki, E., Eklund, P., de Beer, T., Preis, M., Sandler, N., 2018. Handheld colorimeter as quality control tool for inkjet printed flexible levothyroxine doses for pediatric use. *International Journal of Pharmaceutics* 536, 508-509.

Yalkowsky, S.H., He, Y., Jain, P., 2003. *Handbook of Aqueous Solubility Data*, 2nd Edition ed. CRC Press, Boca Raton.

You, M., Lin, M., Wang, S., Wang, X., Zhang, G., Hong, Y., Dong, Y., Jin, G., Xu, F., 2016. Three-dimensional quick response code based on inkjet printing of upconversion fluorescent nanoparticles for drug anti-counterfeiting. *Nanoscale* 8, 10096-10104.

Zhang, J., Feng, X., Patil, H., Tiwari, R.V., Repka, M.A., 2017. Coupling 3D printing with hot-melt extrusion to produce controlled-release tablets. *International Journal of Pharmaceutics* 519, 186-197.

## 7. Figures and Tables

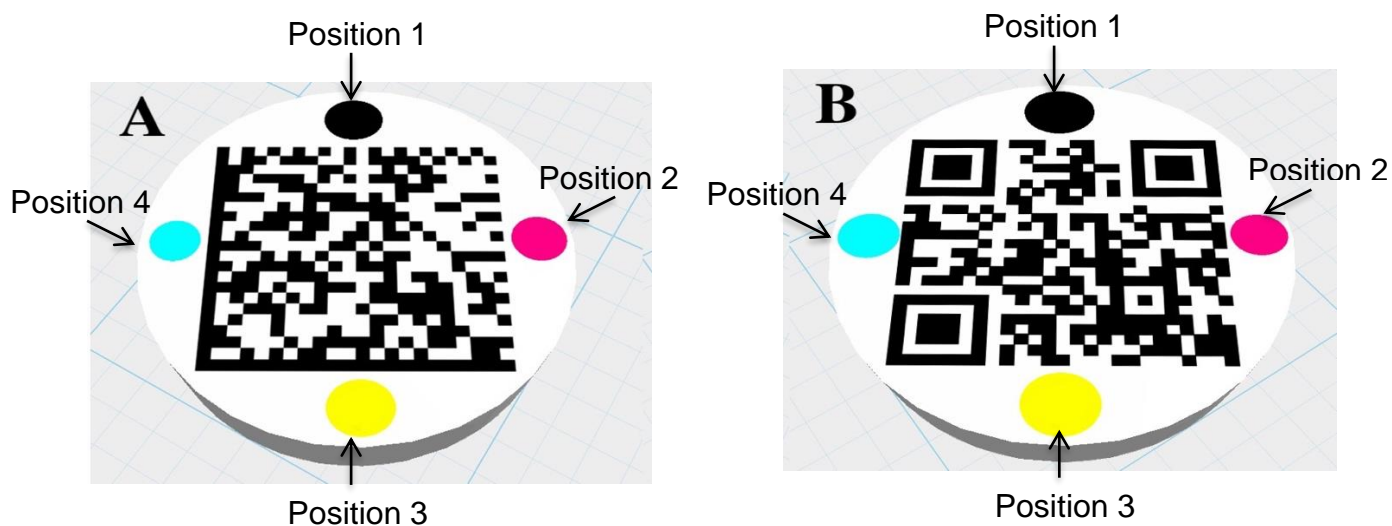


Figure 1. Computer aided designs of anti-counterfeit tablets: (A) Data matrix with anti-counterfeit material deposition (shown as four coloured dots) (B) QR code with anti-counterfeit material deposition (shown as four coloured dots)

Track-and-trace of 3D printed medicines	
<p><b>Treatment information</b></p> <p>Active ingredient/Dose Drug X 100mg</p> <p>Batch N-102276</p> <p>Manufactured by Manufacturing Company</p> <p>Expiry date 15/07/2021</p> <p>Prescribed by and Date Dr A. Smith, 04/01/2019</p> <p>Approved by and Date Ms S. Jones, 04/01/2019</p>	<p><b>Patient information</b></p> <p>Name Ms K. Finch</p> <p>Date of birth 22/08/1974</p> <p>Gender Female</p> <p>Legal Category Prescription Only Medicine (POM)</p> <p>Anti-counterfeit code 1E,2M,3E,4S</p>

Figure 2. Personalized information that was retrieved upon scanning using a handheld smartphone device.

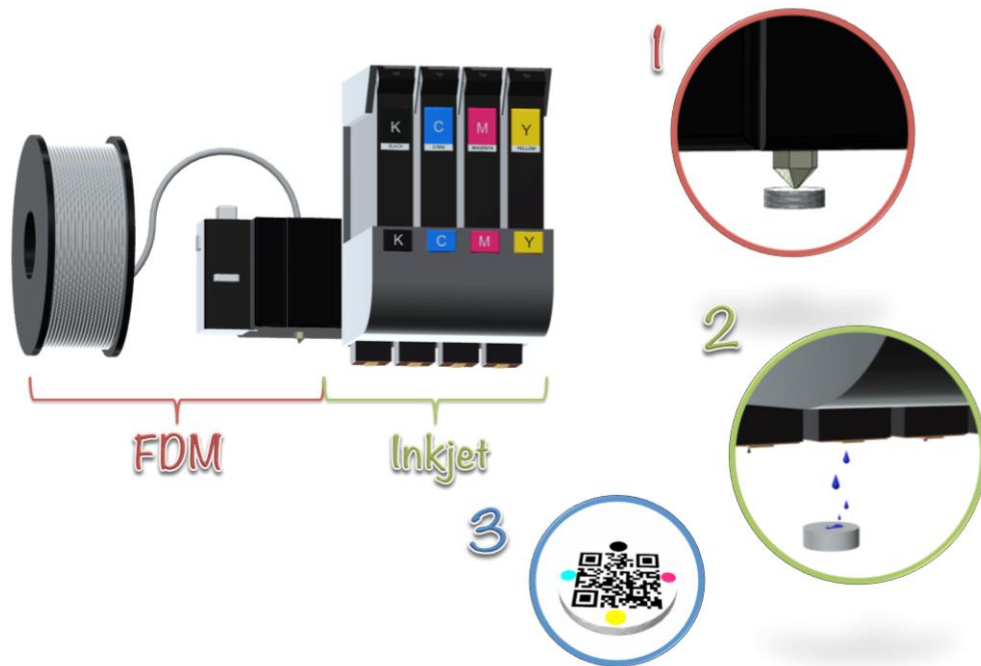


Figure 3. Schematic of combined 2D and 3D printing process for anti-counterfeit measures. Step 1: Extrusion of drug-loaded filament through printhead nozzle; Step 2: Deposition of inks using 2D printing; Step 3: Production of combined personalized medicines with track-and-trace QR code or data matrix and anti-counterfeit material deposition

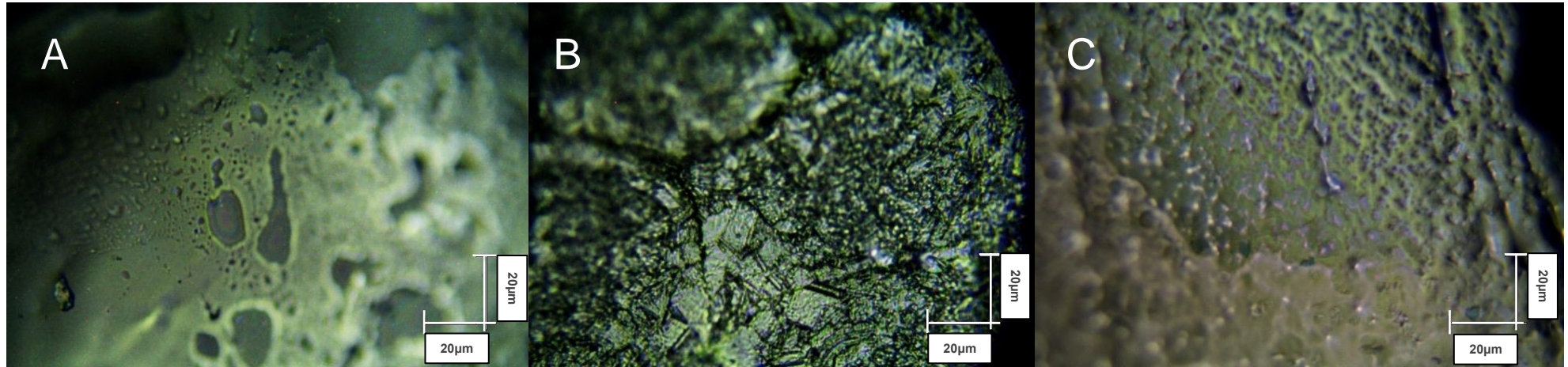


Figure 4. 3D printed tablets with novel anti-counterfeit designs; A) data matrices with model material inks and B) QR codes with model material inks. Scale bar is in cm.

Table 1. Surface tension, dynamic viscosity and density measurements of the prepared inks

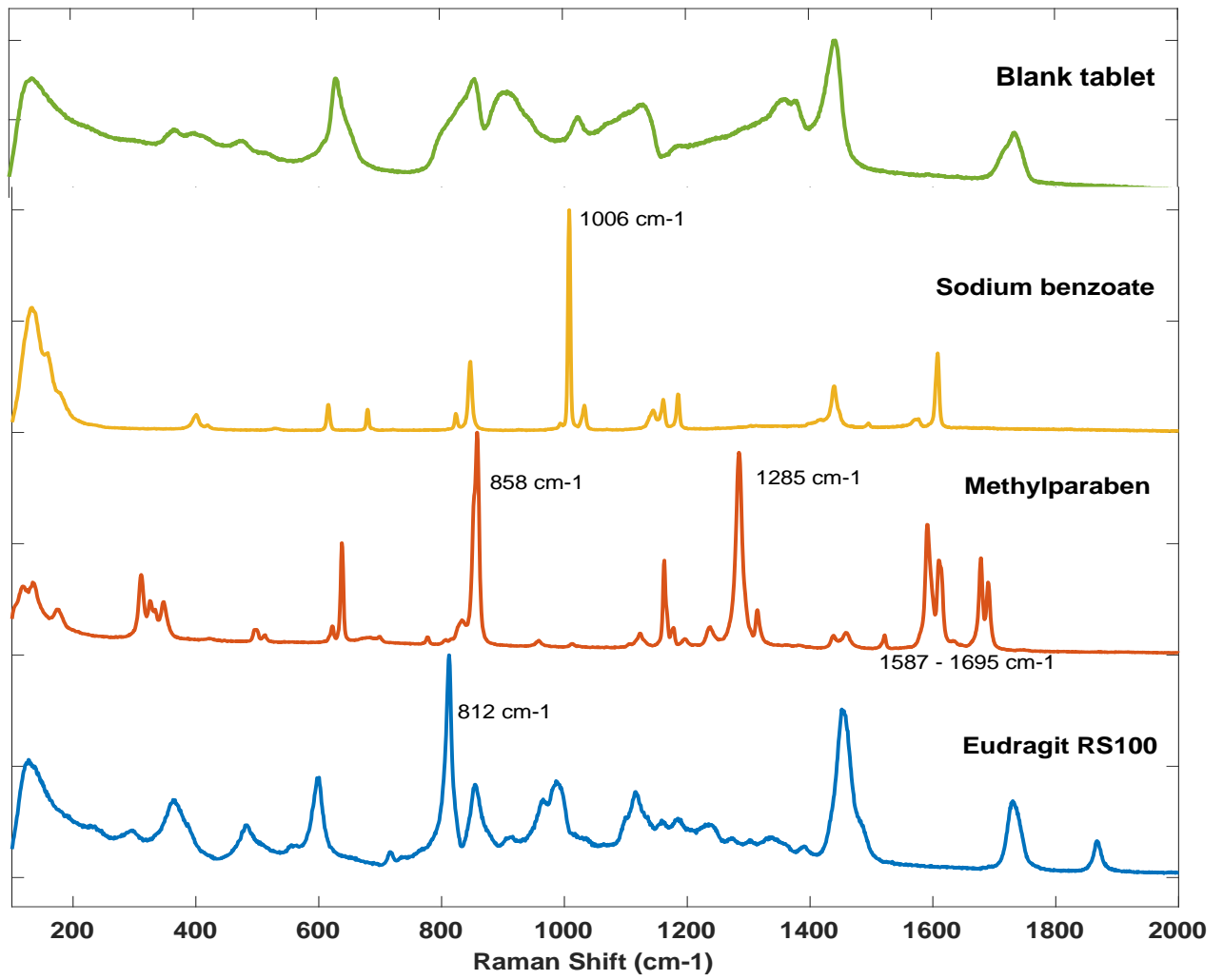
Ink Composition	Surface Tension	Dynamic Viscosity at	Z Value
	(mNm <sup>-1</sup> )	25°C (mPa.s)	
	Mean	Mean	
	± SD	± SD	
Original ink (black)	28.0±1.079	0.93±0.005	4.06
Original ink (cyan)	26.1±0.963	0.97±0.032	3.62
Original ink (magenta)	27.1±0.736	1.03±0.027	3.80
Original ink (yellow)	25.5±0.713	1.04±0.005	3.78
Methylparaben 20% ink	28.3±0.661	1.03±0.049	3.58
Eudragit RS100 10% ink	27.9±0.583	3.31±0.363	1.15
Sodium benzoate 2% ink	27.4±0.763	0.91±0.065	4.58

0

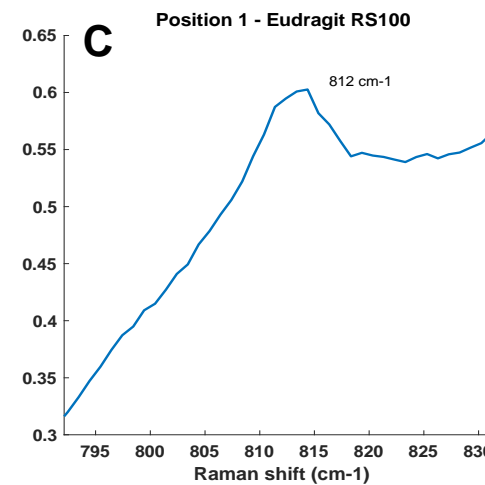
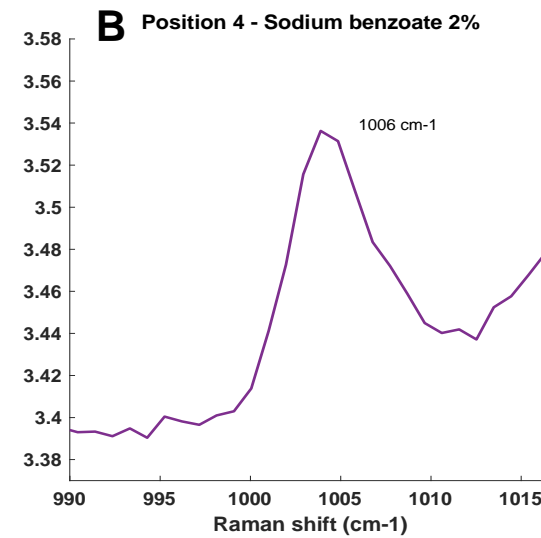
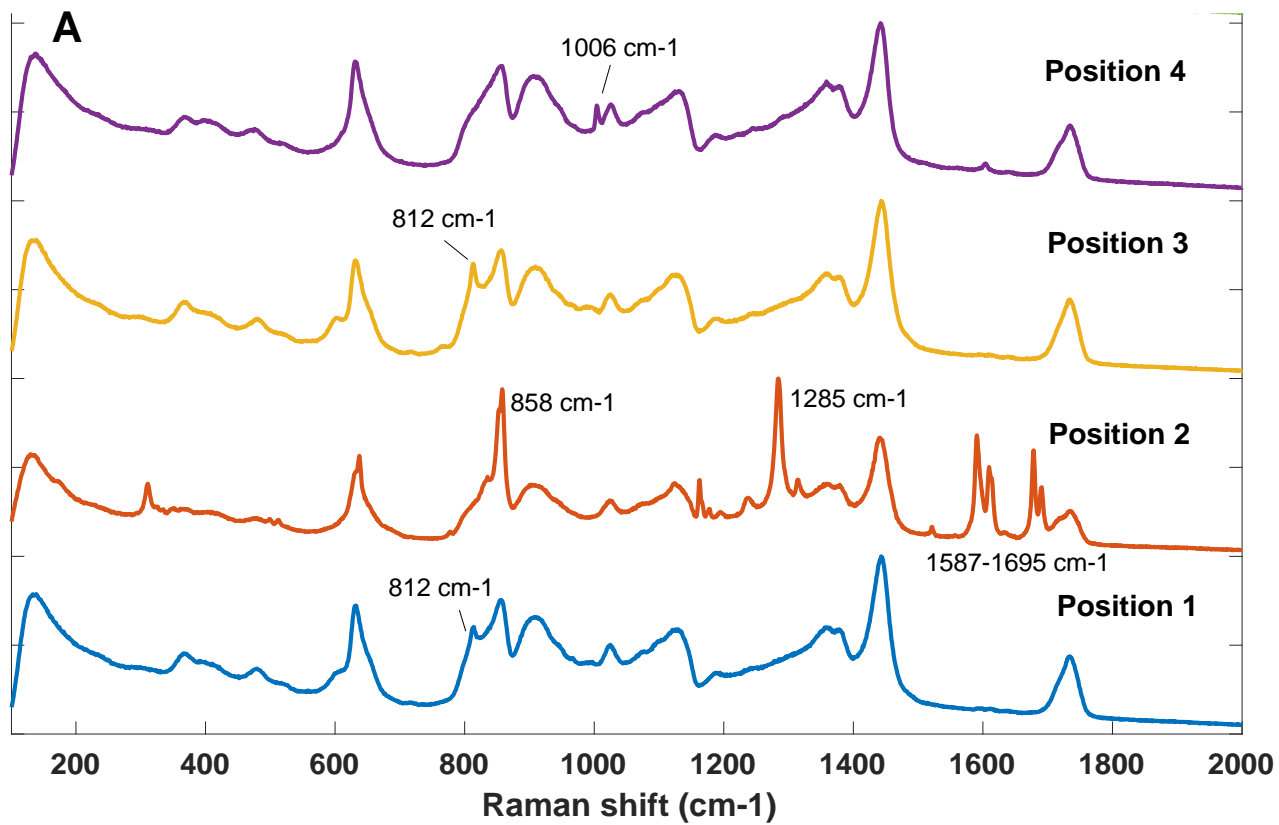


1 Figure 5. Printed material inks viewed under an x50 zoom objective. A) Point 1 (Eudragit RS100 10% ink); B) Point 2 (methylparaben 20%  
2 ink); C) Point 3 (sodium benzoate 2% ink).

3



4 Figure 6. Raman spectra of the raw ingredients of a blank tablet, sodium benzoate, methylparaben  
5 and Eudragit RS100.



6 Figure 7. Raman spectra of the four positions of material inks; Position 1 (Eudragit RS100 ink); position 2 (methylparaben 20 ink); ink); position 3 (Eudragit RS100 ink);  
 7 position 4 (sodium benzoate 2%)

